

Using remote sensing to quantify sediment budget components in a large tropical river – Mitchell River, Gulf of Carpentaria

A. P. BROOKS¹, J. SPENCER¹, J. G. SHELLBERG¹, J. KNIGHT¹ & L. LYMBURNER²

¹Australian Rivers Institute, Griffith University, Nathan, Queensland 4111, Australia
andrew.brooks@griffith.edu.au

²Geosciences Australia, Canberra, Australia

Abstract The recent drought in southern Australia and the increasing realisation that this may be the norm as a result of global warming has led to increased interest in developing the land and water resource of the tropical savannah in northern Australia. Intensive land and water resource development in tropical savannahs in other parts of the world has been shown to lead to significant land degradation, and there are signs this has already occurred with the comparatively moderate levels of historic grazing and agriculture in northern Australia. It is critical that we understand contemporary and historical landscape dynamics before land use is intensified in this region. As a way of beginning to quantify key sediment sources and to start to understand potential changes in relative contributions associated with land use and other drivers, we have begun to construct a sediment budget for the Mitchell River, a 71 360 km² catchment draining into the Gulf of Carpentaria. We present some preliminary results from two key components of the sediment budget: alluvial gully erosion and channel erosion. A remote sensing analysis has identified around 130 km² of active alluvial gullies within the Mitchell megafan, which has an estimated active front length of around 5560 km. Preliminary measurements suggest the average rate of scarp retreat to be 0.34 m per year, with scarp heights ranging between 0.3 and 8 m. Using a spatially distributed method we calculated an annual catchment sediment yield from alluvial gully erosion of >5 Mt/year. Estimates of minimum river channel bed turnover were also determined using a remote sensing approach from Landsat archival data. A measure of minimum annual bed turnover of 15 Mm³/year was derived from analysis of bed area change between 1988 and 2005 (i.e. from either pools to sand bars and *vice versa*, or vegetated island to pools and *vice versa*). When analysed at a tributary scale, these data show a pattern of net sediment scour from the Walsh and Palmer rivers, and net accumulation within all other mainstem channels in the period between 1988 and 2005. These data support the anecdotal evidence that there has been a trend towards sediment accumulation within the lower Mitchell River in recent times, with a resulting net reduction in total pool area of 0.6 km². While preliminary, these data highlight the value of remote sensing for constructing sediment budgets in large dynamic tropical rivers.

Key words sediment budget; Mitchell River; alluvial gully erosion; bed load; remote sensing; Landsat; ASTER

INTRODUCTION

The relationship between European land-use enhanced sediment supply to rivers in southern Australia, compared with late Holocene rates, is now well established (e.g. Brooks & Brierley, 1997; Rutherford, 2000; Prosser *et al.*, 2001). Gully and bank erosion have been highlighted as disproportionate contributors to sediment budgets in this region (e.g. Olley *et al.*, 1993; Brooks *et al.*, 2003; Wallbrink, 2004), with assumptions that this is also the case for the rest of Australia. Accelerated sediment supply has been shown to be a function of one or more disturbance processes: upland and riparian forest clearance, grazing, agriculture and river engineering (e.g. Erskine & Green, 2000; Rutherford, 2000; Brooks *et al.*, 2003).

With climate change predicted to cause significant drying of southern Australia, further impacting the already massively over-allocated rivers, many are now looking for new land and water resources to develop in tropical northern Australia, to make up the shortfall in the south. Yet, if northern Australia is to be developed without repeating the mistakes that were previously made in southern Australia, there needs to be a rapid improvement in our understanding of some fundamental landscape processes before the development process begins, especially with regards to erosion and land use in the past, present and future. While some consider much of northern Australia relatively “pristine” (e.g. Woinarski *et al.*, 2007), land degradation from cattle grazing on savannah plains, altered fire regimes, alluvial and hard-rock mining, and localized intensive agriculture have already altered many processes and conditions (e.g. Crowley & Garnett, 2000;

McDonald & Dawson, 2004). Therefore, to understand the potential impacts of *increased* development in northern Australia, we must first quantify the changes that have *already occurred*.

This study focuses on the Mitchell River, a large (71 360 km²) catchment that drains from the eastern highlands of North Queensland into the Gulf of Carpentaria (Fig. 1), and has one of the highest mean annual discharge volumes in Australia (>8 000 000 ML/year, excluding the Alice River). The Mitchell catchment is an ideal area to assess the typical array of land use found across northern Australia: cattle grazing, altered fire regimes, alluvial gold mining, hard-rock mining, and some locally intensive irrigated agriculture and horticulture. Anecdotal evidence suggests that: (1) large pools within the lower Mitchell River have gradually infilled due to historic catchment disturbance; and (2) gully erosion has increased across savannah plains. Aerial reconnaissance around the catchment in 2004 supports these hypotheses, identifying two key processes that could be giving rise to accelerated erosion: (1) alluvial gold mining of channel bed deposits within one major tributary – the Palmer River; and (2) extensive areas of alluvial gully erosion within the Mitchell fluvial megafan (*sensu* Leier *et al.*, 2005).

The Mitchell fluvial megafan is the largest in Australia (31 000 km²) and is dominated by unconsolidated alluvial silts and clays. It was described in detail by Grimes & Douth (1978), who defined and delineated distinct fan units that coalesced and prograded seaward through the Pliocene, Pleistocene and Holocene. We extend this work by analysing the spatial patterns of different erosion processes within the megafan, and using the fan evolutionary framework to provide insight into the erosion processes. In this paper we describe our initial work toward the development of a sediment budget for the Mitchell catchment, focusing initially on two major components of the budget – alluvial gully erosion and channel erosion. *Alluvial gully erosion* has been defined as a distinct class of gullying by Brooks *et al.* (2008), who also describe in more detail the morphology and process of deposition and erosion on the Mitchell megafan.

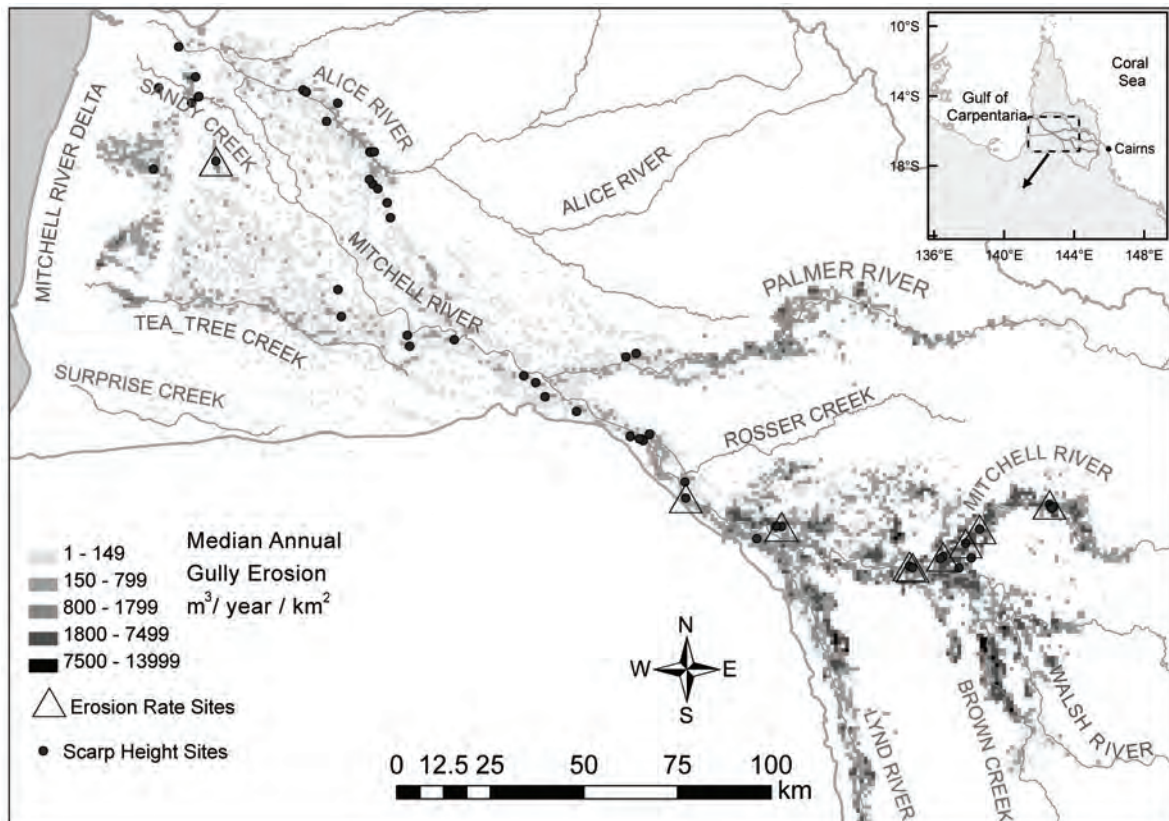


Fig. 1 Location map of Mitchell catchment, showing distribution and rates of alluvial gully erosion across the lower megafan, and location of erosion scarp height and rates sites.

Previous sediment budget approaches in relation to gullying

The application of a sediment budget approach (*sensu* Dietrich & Dunne, 1978) and more recent computational models such as SedNet (e.g. Prosser *et al.*, 2001) are now well developed geomorphic approaches for assessing relative contributions of sediment sources at the catchment scale and changes in these contributions through time. When quantifying specific sediment sources like gully erosion, the traditional approaches have been either to conduct field surveys or to manually map gullies within the catchment from aerial photographs (e.g. Ionita, 2006). However, these approaches are only practical in small catchments. Alternatively, for large catchments, geostatistical modelling has been used to extrapolate from a sample area (mapped at high resolution from aerial photographs) to the whole catchment (e.g. Wilkinson *et al.*, 2005). Increasingly, these mapping and modelling approaches are being complemented with radionuclide and mineral tracing techniques (e.g. Rustomji *et al.*, 2008). A limitation of the geostatistical approach is the dependence on the existence of strong relationships between geomorphic metrics (e.g. slope, area and relief) and erosion (e.g. colluvial gullies). Furthermore, geostatistical modelling is highly dependent on the availability of high-resolution spatial data on soils, topography, vegetation, rainfall and runoff. In a large, data-poor catchment like the Mitchell River, where a major part of the catchment is relatively flat, and where there is an atypical relationship between topography and alluvial gully distribution (see Brooks *et al.*, 2008), a geostatistical approach based largely on slope and topography is not appropriate. Instead, we have utilized remote sensing to map alluvial gully distribution throughout the alluvial portion of the catchment, where this type of gullying occurs.

Spatial analysis of bed load dynamics

The mainstem channels of the Mitchell and its tributaries are large “bimodal channels” with a sinuous and often multi-thread low-flow or dry-season channel, inset within a larger macro-channel (*sensu* van Niekerk *et al.*, 1999), which conveys much larger wet season flows (Fig. 2).

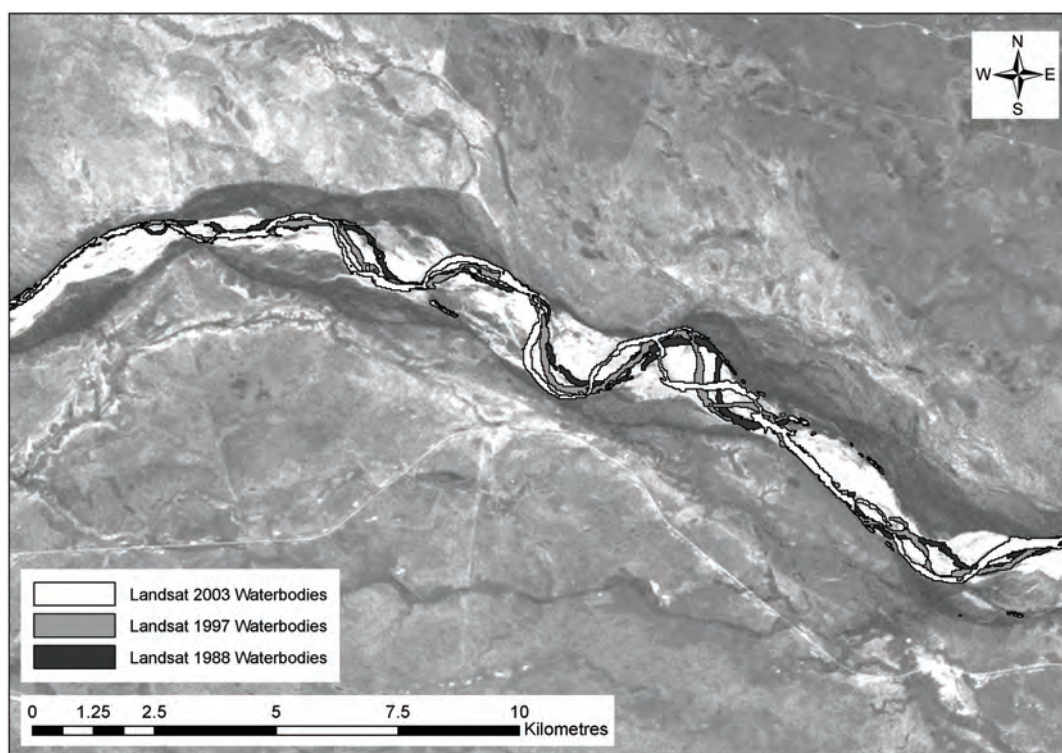


Fig. 2 Landsat image showing the shifting location of pools in the Mitchell River low-flow channel between 1988, 1997 and 2003. The macro channel can be seen as the area defined by the darker riparian vegetation.

The location of the low-flow channel (thalweg) is highly dynamic over time, resulting in a shifting habitat mosaic (*sensu* Stanford *et al.*, 2005) of in-channel riparian vegetation communities, within macro-channels up to 2 km wide that in places are incised into the megafan deposits. Sediments deposited within the macro-channel tend to be bed load sands and gravels. Hence, mapping the shifting of geomorphic units within the macro or “active channel zone” can provide insight into the bed load turnover, as a proxy measure of minimum bed load transport (*sensu* Ham & Church, 2000). It was assumed that vegetation change in this area is a function of fluvial reworking rather than any other disturbance, and consequently inferences can be made about sediment turnover from detected vegetation changes. Ham & Church (2000) highlight the advantages of using a spatial mapping approach, in their case using aerial photographs, to determine the bed load budget at reach scales (e.g. 10s of km), over traditional sediment transport modelling and measurement methods. Others have applied a remote sensing approach to sediment budgeting at the scale of large river reaches (several 100s of km) (Aalto *et al.*, 2008). Thus, a remote sensing approach is the only practical method for measuring channel change through time at the catchment scale in a large river like the Mitchell, and hence beginning to quantify the contribution of channel erosion (i.e. the reworking of in-channel bars, benches and islands, as well as bank erosion) to the overall sediment budget.

METHODS

Alluvial gullying

Remote sensing and mapping Mapping of alluvial gully erosion in the Mitchell River catchment was undertaken using 10 ASTER scenes, subset to extents covering the Mitchell River megafan, excluding the marine influenced deposits in the delta. The megafan limits were delineated from a surface geology data set that describes the extent of flood plain and channel alluvium at 1:1 000 000 (Whitaker *et al.*, 2006), as well as the 1:2M soil landscapes data set (BRS, 1991).

The image data were acquired at various times between September 2000 and October 2004 and bands 1–9 were used in the analysis covering the green, red, near infrared (NIR) and mid-infrared (SWIR) wavelengths. A ground resolution of 15 m × 15 m pixels was derived for all bands by resampling the mid-infrared bands from 30 m to 15 m (prior to purchase). A Principal Components Analysis (PCA) data set was derived from the 9-band ASTER data set. A Normalised Difference Vegetation Index (NDVI) layer was also derived from the ASTER red and NIR bands. All 19 layers (ASTER, PCA and NDVI) were stacked for a scene. Initially, an analysis of which data layers to use as input to gully processing was undertaken by comparison of histograms from a small subset of field mapped gullies using all 19 data layers. As a result, the optimal layer combinations from which to distinguish between gully and other terrain units was found to be five layers including ASTER-Green, NDVI, and PCA bands 2 and 5. These five layers were used as input to the subsequent processing, where delineation of alluvial gullies was achieved using a decision tree classification approach. Each scene was processed separately due to differences caused by acquisition time differences (across both seasons and years). The decision tree analysis involved a sequence of threshold splits calibrated using *in situ* GPS survey data of gullies, a suite of 3028 aerial photos and Lidar data acquired in 2006 that targeted specific gullies on the megafan. For the decision tree process, each level of the decision tree was modified (tweaked) for each scene to adjust for the inter-annual and seasonal differences between scenes. After processing all 10 scenes, the derived gully layers were mosaiced. The resultant gully layer was then converted from raster (pixel) data to vector (polygon) data using an exact pixel to vector transform.

Validation

Gully detection and size Validation of the alluvial gully mosaic was undertaken using two approaches both of which utilized publicly available Google Earth “Quickbird” imagery. For an assessment of the detection of gullies across the Mitchell megafan, the Quickbird scenes, available

online and coincident with the megafan, were gridded in 1-km cells. The grid covered 15 120 km², representing 47% of the megafan. From these a subset of 250 randomly selected 1-km cells were visually assessed for alluvial gully presence or absence, and compared with the ASTER-derived gully presence/absence data to provide an assessment of gully detection accuracy (true/false positives; true/false negatives). The second validation approach involved randomly selecting 83 1-km cells from within the available Quickbird 1-km grid, which also contained mapped ASTER gullies. Gullies viewable in Quickbird were digitized and their area and perimeter calculated in ArcMap. Quickbird gully area was then compared to ASTER gully area and perimeter for gullies found within each of the 83 grid cells.

Length of gully front Using the same 83 1-km grid cells as above, alluvial gully fronts and head scarp locations were mapped from the Quickbird imagery. The total length of Quickbird gully fronts in each 1-km cell was then compared to the total perimeter length of gullies mapped via ASTER. For each 1-km cell, a ratio of Quickbird to ASTER length was calculated. The total length of gully front via Quickbird (km/km²) was used to adjust the total length of ASTER perimeter (km/km²). Validation of gully front lengths measured from Quickbird imagery amounted to comparing the mapped gully front length to field data at sites where detailed differential GPS field surveys had been conducted (total 25 485 m, Table 1). The ratio of the ground surveyed to remote sensing surveyed gully front lengths were then used to adjust ASTER and Quickbird gully front length estimates.

Erosion rates at gully fronts Detailed surveys of selected alluvial gully fronts in the Mitchell megafan were conducted using *in situ* differential GPS with sub-meter accuracy (Trimble with Omnistar HP). Accuracy depended on signal strength and vegetation cover, but obtained results were typically within 0.5 m for repeat surveys of stationary locations. GPS surveys were conducted at nine sites across the alluvial megafan, totalling 25 485 m of gully front surveyed repeatedly (Table 1 and Fig. 1). Average scarp retreat rates of gully expansion were determined from annual surveys in 2005, 2006 and 2007, with the average rate equalling the total erosion area of change during any given year divided by the total survey length. Maximum linear rates were calculated for individual lobes, but only the average rate was applied across the entire length for budget purposes (Table 1).

Scarp heights at gully fronts Near-vertical scarp heights at gully fronts were estimated using both field and remotely sensed data. It was assumed the majority of new sediment contributed to the gully each year comes from the portion of the gully undergoing vertical scarp retreat (as

Table 1 Surveyed lengths and erosion rates at alluvial gully head scarps sites.

Years	Site ID	Survey length (m)	Max retreat (m/year)	Mean retreat (m/year)
2006–2007	MMGC1	832	8.13	0.10
2005–2006	MMGC1	773	6.50	0.32
2006–2007	WPGC1	554	2.03	0.03
2006–2007	WPGC2	6782	10.26	0.38
2006–2007	WPGC3	4140	6.60	0.30
2005–2006	WPGC3	2534	8.09	0.09
2006–2007	GBGC1	1525	1.32	---
2005–2006	GBGC1	1431	1.93	---
2006–2007	GBGC2	969	14.10	0.82
2006–2007	GBGC3	1843	4.51	0.65
2006–2007	HBGC1	1763	3.85	0.53
2006–2007	KWGC1	2339	3.20	0.36
Total		25 485		
Median (50)			5.51	0.34
25th percentile			2.91	0.15
75th percentile			8.10	0.49

opposed to secondary reworking of material deposited with the gully). Airborne Lidar surveys of gullies were conducted in 2006 at four sites across the megafan. Within each Lidar site, three longitudinal profiles of gully channels were surveyed, to calculate the height of the near-vertical scarp. To supplement these data, field measurements of scarp height were collected during soil sampling at scarps. In combination, these data were used to develop a distribution of gully scarp heights across the megafan. Due to variation in scarp height along the profile of the Mitchell River and megafan, scarp height data were stratified by flood-plain elevation derived from a 30-m SRTM DEM.

Sediment budget calculations Annual sediment production calculations for alluvial gullies were performed at a 1-km² grid scale across the portion of the megafan covered with gullies. Average scarp height within any one cell was estimated from the relationship between scarp height and flood-plain elevation. ASTER-derived gully-polygon perimeter data per km² were used to estimate the density of gullying in each 1-km grid cell. The ASTER gully perimeter data were adjusted to ground scarp lengths using relationships between Quickbird/ASTER and GPS/Quickbird length data. For both the distributions of Quickbird/ASTER lengths and GPS/Quickbird lengths, the median and 25th/75th percentile ratios were extracted to use in sediment budget calculations, in order to propagate potential error through the budget. Since erosion rate data represented considerable ground distances but were not spatially well distributed across the catchment, these data were not stratified at the 1-km grid scale or megafan sub-regions, but were applied across all sites using the median and 25th/75th percentiles.

Bed load dynamics

To estimate annual bed material turnover in the main stem channels of the Mitchell catchment (i.e. the channel network depicted by the 1:5 million scale drainage network – see Fig. 2), a standard remote sensing change detection approach was used. Landsat Thematic Mapper (TM) mosaics produced by the Queensland Government Statewide Landcover and Tree Study (DNRW, 2008) from 1988 and 2005 covering the mainstem channels were assessed for changes in vegetation, in-channel sand deposits and low-flow in-channel water bodies (i.e. pools). In total, 3528 km of channels across the catchment were assessed in order to demonstrate the approach in a large catchment.

Processing and analysis of the Landsat TM imagery The active channel zone was manually delineated from the Landsat TM mosaic for all channels defined by the 1:5 million drainage network based on a visual assessment of 2005 imagery. Vegetation with a denser canopy cover than the surrounding landscape, including distinct fluvial features such as bars, benches, islands and water holes were included in the active channel zone. Ecognition (version 4) image processing software was used to segment the delineated in-channel areas identified from the Landsat TM data into image objects representing discrete features including vegetated in-channel island, unvegetated sand bars and water. An object oriented classification approach, such as in Platt & Rapoza (2008), was used in preference to a pixel based classification approach because land cover types such as open forest that exhibit considerable within class variability can be more easily differentiated from other highly variable but different classes. A training exercise was applied to 14 strips of airborne tri-spectral scanner data acquired in 2006 (described in Brooks, *et al.*, 2006) and 824 training polygons were collected from within the active channel zone, and these data used to seed a nearest neighbour classification within Ecognition and then used to classify objects based on their reflectance characteristics from all six bands of Landsat TM data.

To assess the accuracy of the polygons mapped from the 2005 Landsat imagery, 16 strips of tri-spectral scanner data were examined and an additional 1183 polygons selected to assess the accuracy of the classification. This was done using the same process as the training data, but using different tri-spectral scanner data. The same classification process was applied to the 1988 imagery as for the 2005 imagery on the assumption that the spectral responses of the broad land cover classes were stable in Landsat TM data over time.

Table 2 Summary table showing the underlying geomorphic implications of the observed changes indicated by the remote sensing data. Only those categories from which an unambiguous interpretation can be made of scour or deposition have been used in subsequent calculations.

Nature of change 1988–2005	Physical interpretation of detected change
Veg to Veg, Sand to Sand, Water to Water	Status quo (i.e. no discernible net change). However veg density may have changed and sand–sand and water–water likely includes major turnover
Veg to Sand	Possible island or bench scour (ambiguous)
Sand to Veg	Island/bar formation + stabilisation (ambiguous)
Water to Sand	Bar formation (= deposition)
Water to Veg	Island/bar formation + stabilization (= deposition)
Sand to Water	Bar scour (= scour)
Veg to Water	Erosion of vegetation and bar scour (= scour)

Change detection 2005–1988 To determine the gross channel changes over the 17-year interval (1988–2005), a change detection analysis was performed (*sensu* Milne, 1988) between the three basic land cover classes (vegetation, sand and water) that allowed us to interpret channel morphodynamics. For the purposes of understanding channel dynamics, a more complex delineation of vegetation community classes was simplified to a super class of vegetation. In reality the vegetation classes predominantly represent vegetated in-channel bars and benches. While channel dynamics are complex, we have synthesized the change scenarios down to three fundamental geomorphic changes: (1) channel scour; (2) in-channel deposition; or (3) no net change (Table 2). The observed changes only reflect a two-dimensional change, and so it is only by inference (and knowledge of processes on the ground) that we have attributed geomorphic responses to the observed changes. Field observations in the Mitchell River indicate that if a pool is infilled to become a sand bar (or the converse), somewhere in the order of 3–10 m of deposition (or scour) has taken place at that particular site. Assuming this as typical, estimates of the minimum depth of bed material that has been turned over to either deposit a bar or scour a pool can be made, and hence derive estimates of minimum sediment turnover within the channel. The assumption is also made that in the *status quo* category, on average, there has been no net change in sediment storage. However, the extent to which any sand bar has been turned over or exchanged from one wet season to the next is unknown. As such, a sand bar may be mapped similarly at the two time intervals (1988 and 2005), but may have been scoured and redeposited every year of the intervening period. As a result, the volumetric calculations are conservative. In reality, sand bars are likely to be the most active parts of the channel, given that vegetation has not been able to colonise these surfaces.

RESULTS AND DISCUSSION

Alluvial gullying

Detection of gullies by the ASTER remote sensing method varied due to both ASTER scene differences and differences in size and reflectance of individual alluvial gullies. Validation of ASTER-based gully mapping using 250 randomly selected 1-km cells, the ASTER image detected 45 (18%) false positives and 18 (7%) false negatives. These results indicate that classification errors can occur when using remote sensing to detect alluvial gullies. False negatives were a result of lack of resolution in the ASTER and ability to detect gullies in heavily vegetated areas. False positives represented the detection of either: (1) highly scalded surfaces stripped of their shallow A-horizon and grass vegetation; (2) the bed of small, dry seasonal wetlands; or (3) road surfaces. Overall however, the ASTER classification was very successful in detecting the larger alluvial gully complexes between 1 ha and 1 km².

Table 3 Alluvial gully erosion extents, rates and sediment production.

Gully parameter	Median	25%	75%
Total area gullies (km ²) (ASTER)	167	–	–
Total area gullies (km ²) (Adjusted from Quickbird)	129	–	–
Perimeter gullies (km) (ASTER)	13 080	–	–
Perimeter gullies (km) (Adjusted from Quickbird)	4840	650	12 000
Perimeter gullies scarp front (km) (Adjusted from GPS)	5570	680	16 000
Average gully erosion rate (m/year)	0.34	0.15	0.49
Total annual erosion volume (m ³ /year)	3 170 000	171 000	13 376 000
Total annual erosion (tonnes/year) (assume 1600 kg/m ³)	5 070 000	273 000	21 401 000
Median annual gully erosion volume per km ² (m ³ /year/km ²) (of 1-km grid cells with gullies – Fig. 2)	100	5	420
Denudation rate of megafan (mm/1000 years) (31 000 km ²)	100	6	430

After the initial validation exercise, false positive roads across the entire megafan were manually removed from the data set, representing a 28 km² reduction in ASTER detection area. The remaining error was corrected for via the Quickbird validation procedure, where gully area, gully perimeter and scarp length adjustments were applied from the data derived from the 83 randomly selected 1km cells manually digitized at high resolution. For the ratio of Quickbird scarp length to ASTER perimeter using the 83 1-km cells, the median ratio applied was 0.37 with a 75th percentile of 0.93 and 25th of 0.05. Thus, ASTER perimeter estimates consistently overestimated gully front scarp lengths. Also, the ground surveyed GPS lengths were greater than Quickbird estimated scarp lengths (median ratio of 1.15, and a 75th percentile of 1.34 and 25th of 1.04), also attributed to the higher resolution of the *in situ* surveys.

Measurements of maximum erosion rates along surveyed gully fronts varied by site and by specific alluvial gully lobe (Table 3). Only a small proportion of lobes displayed significant amounts of retreat activity when compared to the whole scarp length. For example, at two sites (WPGC 2 and 3), a cumulative 17% of the scarp length showed measurable signs of retreat, albeit significant (up to 10.26 m/year) in certain locations. For sediment budget purposes, the average retreat rate across the entire scarp length was used (Table 3).

In order to estimate scarp heights (S_h) at gully fronts, a relationship was developed from the flood-plain elevation (E_l) adjacent to a gully (using 30 m SRTM DEM data), as in equation (1), with $r^2 = 0.77$.

$$S_h = 0.0004E_l^2 - 0.0509E_l + 1.8373 \quad (1)$$

Flood-plain elevation decreased relatively consistently down the longitudinal profile of the megafan, while scarp height varied with the relative relief between the river channel and flood plain. Thus, where the river was incised into the upper part of the megafan, the flood-plain elevation, relief and scarp height were greatest. Both relief and scarp height decrease downstream toward the current hydrological apex of the megafan, below the Palmer River junction (Fig. 1), where scarp height was the lowest. Scarp height increased again toward the delta and Sandy Creek, possibly due to hydroisostatic warping or backwater deposits behind beach ridges (Chappell & Rhodes, 1982).

For each 1-km cell across the megafan, the scarp height was estimated from equation (1). Scarp lengths were estimated from the density of ASTER polygon perimeters and ratio scaling factors between ASTER, Quickbird, and GPS lengths. A uniform scarp retreat rate was applied across all 1-km grid cells. The median and 25th/75th percentiles of these data (not normally distributed) were used to calculate best estimate and error margins around volumetric gully erosion rates. These estimates have been reported in Fig. 1 and Table 1. Median annual alluvial gully erosion rates (m³/year/km²) varied systemically across the megafan and were largely controlled by the density of gullies and local scarp height. As a result, the largest erosion rates were located near the Mitchell-Walsh confluence (Fig. 1) and upper Palmer, where the river channels have incised

into megafan deposits. Erosion rates decreased downstream below the Palmer confluence at the current hydrological fan apex, but increased again near the delta where scarp heights increase again.

Estimates of the median total annual erosion volume (m^3/year) (Table 3) were quite high at 3 million m^3 per year; however, the 25th and 75th percentile values varied from this median by an order of magnitude. The 25th and 75th percentile values highlight the uncertainty in the data and analysis technique used. They also highlight the difficulty in accurately quantifying the major component of a sediment budget in large complex catchments like the Mitchell. Nevertheless, it is only through a spatial analysis like this, coupled with an extensive field data set, that we can represent the error inherent in these sediment budget calculations.

Bed load turnover

The data presented in Fig. 3 show the trend in net sediment accumulation or scour at the scale of the major sub-catchments. In an attempt to acknowledge some of the “known unknowns” we have incorporated an upper and lower estimate of turnover depths, along with our best estimate (Table 4). Despite, these data only representing net change between two time slices, across a 17-year interval, they demonstrate a clear trend towards net accumulation in some sub-catchments and net scour in others. The graph has been separated into the two components of scour and deposition that we can be confident does represent change. Of these the sand–water and water–sand classes are the least ambiguous, and because, by definition, it excludes any of the channel impacted by riparian vegetation, should highlight any broad trend towards either pool in-filling or increasing pool area.

The two most extensive areas of in-channel zone, the upper Mitchell and the Mitchell fan reach, would appear to be in equilibrium, as indicated by the roughly equal areas of scour (sand–water) and bar deposition (water–sand) shown in Fig. 3. In fact, the scale of this graph actually masks a net increase in pool area within the upper Mitchell of 0.39 km^2 , and a net increase in sand bars of 0.58 km^2 within the Mitchell fan reach. While both figures represent a small proportion of the total zone area, in absolute terms they represent substantial areas of net change. When the other two categories are included (veg–water; water–veg), the trend in the upper Mitchell is reversed, indicating a net accumulation area of 9.23 km^2 , while the trend in the lower Mitchell is enhanced, indicating there has been a net increase of 3.89 km^2 of channel area in which sediment has accumulated. The ambiguity in the upper Mitchell is likely a function of the sub-catchment delineation used for the sub-catchment in this analysis. Regardless, these data would tend to support the anecdotal evidence within the lower Mitchell River, that there has been a trend of pool infilling within recent history. The trend in the upper Mitchell is more ambiguous, and would require analysis at a higher spatial and temporal resolution to determine the precise trend.

Of the other tributaries, both the Walsh and Palmer have experienced a 1.53 and 1.32 km^2 net increase in pool area, respectively, suggesting there has been net export of sediment from these streams. The trend is somewhat dampened, however, when the other two change classes are included in the analysis, with the net area of channel indicating sediment loss now being only 0.32 and 0.75 km^2 , respectively. The Alice and Lynd rivers, alternatively, demonstrate a net increase of 0.97 and 0.35 km^2 , respectively, in the aerial extent of in-channel sand bars, when considering just the sand–water–sand dynamics. When all classes are included this trend is further enhanced in both cases (3.69 and 1.98 km^2 , respectively).

These data would appear to indicate that, at the overall catchment level, there are some distinct patterns in the way different tributaries are behaving through time. One way of interpreting these data is that the Walsh and Palmer have seen a net export of sediment over the last 17 years, possibly reflecting the reworking of mining related sediment pulses delivered to each tributary over the last century. The Lynd and Alice rivers, however, would appear to have experienced net sediment accumulation. Without further evidence of sediment sources we can only speculate at this stage on what might be the drivers of these changes, but it is likely a combination of the differing geology and flood regimes in each tributary, coupled with the different land-use intensity, particularly the grazing and fire regime.

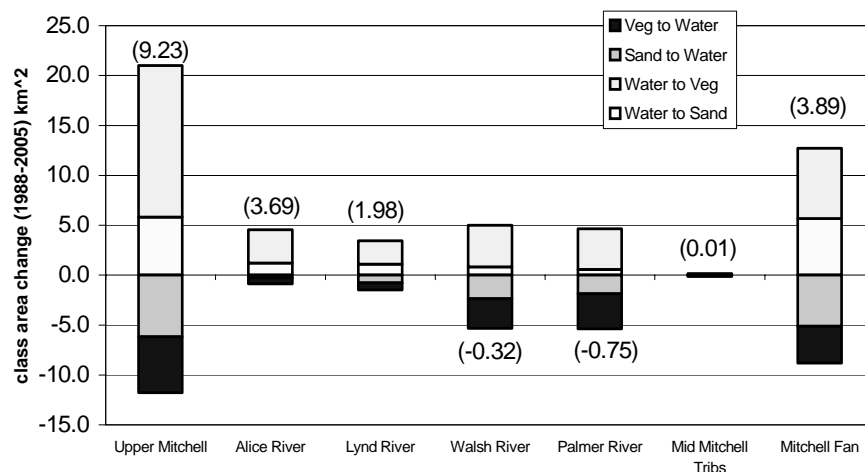


Fig. 3 Relative change in the aerial extent of scour (sand–water) + (veg–water) and deposition (water–veg) + (water–sand) within the active channel zone between 1988 and 2005 in the main Mitchell tributary sub-catchments. See Fig. 1 for tributary locations. The Mitchell Fan reach is downstream of the Palmer River confluence, while the upper Mitchell is the main-stem channel upstream of this point. The mid-Mitchell tributaries are a combination of Brown and Rosser creeks. The assumption is made that the water detected in the dry season imagery in both years represents pools in which water depth is several metres or more in depth. The area of net scour and deposition is shown in brackets within each sub-catchment segment. Positive change represents deposition and negative change represents scour.

Volumetric changes

To translate the observed changes in aerial extent of the various classes into volumes of net scour and deposition, and hence bring them into the standard currency used in sediment budgeting (sediment volume), we need to know something about the likely depths of both scour and deposition. As discussed above, only rough field estimates exist, and improving these estimates is the subject of ongoing field work. As outlined in Table 4, we have derived three estimates of channel turnover volume for average scour depths of 1, 3 and 5 m. The total annualized turnover

Table 4 Volumetric calculations of sediment accumulation and scour by sub-catchment. Only the four classes highlighted are used for determining the net scour or deposition, given that they are the only unambiguous classes. Extensive volumes of sediment turnover are also likely to be occurring within the other classes, particularly sand–sand, but without scour depth data we are unable to constrain these volumes. Consequently the volumes represented are absolute minima.

+	(Units = km ²)	Upper Mitchell	Alice River	Lynd River	Walsh River	Palmer River	Mid Mitchell Tribs	Mitchell Fan	Total
1	Water to Sand - deposition	15.19	3.33	2.35	4.18	4.08	0.13	7.02	36.27
2	Water to Veg - deposition	5.81	1.23	1.11	0.83	0.56	0.01	5.69	15.24
3	Sand to Water - scour	5.57	0.61	0.73	2.96	3.51	0.09	3.71	17.17
4	Veg to Water - scour	6.20	0.26	0.76	2.37	1.87	0.04	5.11	16.61
5	Sand to Veg	17.03	12.53	12.64	7.83	8.13	4.19	14.01	76.35
6	Veg to Veg	45.93	9.62	20.56	20.23	25.38	2.75	35.23	159.70
7	Water to Water	15.46	0.49	1.19	3.37	2.72	0.07	16.57	39.87
8	Veg to Sand	6.94	1.91	6.84	3.38	2.36	0.49	4.01	25.93
9	Sand to Sand	31.37	8.43	28.79	9.59	7.25	2.70	40.39	128.52
10	Total ch area								515.66
11	Total area turned over (sum row 1:9)	32.76	5.43	4.94	10.33	10.02	0.27	21.53	85.30
12	Annual turnover (row 11/17)	1.93	0.32	0.29	0.61	0.59	0.02	1.27	5.02
13	Sediment turnover (m ³)								
14	Turnover vol (low = 1m av scour)	1 927 279	319 228	290 846	607 868	589 485	15 919	1 266 728	5 017 353
15	Turnover vol (med = 3m av scour)	5 781 838	957 684	872 537	1 823 603	1 768 456	47 757	3 800 184	15 052 059
16	Turnover vol (high = 5m av scour)	9 636 397	1 596 140	1 454 228	3 039 338	2 947 426	79 596	6 333 640	25 086 765
17	Net total change km ² (1+2) – (3+4)	9.23	3.69	1.98	–0.32	–0.75	0.01	3.89	17.72
18	Net annual change m ³ (1+2) – (3+4)	1 628 162	650 404	348 640	–56 250	–131 912	1 213	686 801	3 127 059

(i.e. scour + deposition) for the intermediate estimate is around 15 Mm³. Interestingly, the net volume change (deposition – scour: calculated from the medium scour depth estimate) of 3.1 Mm³/year is very similar to the calculated median annual sediment contribution from alluvial gully erosion. This is not to suggest the two are necessarily related, as the gullies are generally contributing suspended sediment, but it suggests we are dealing with appropriate orders of magnitude of sediment contribution from these two sources, and that there is a major trend towards net in-channel aggradation within the lower Mitchell River.

CONCLUSION

Deriving sediment budgets for large, remote tropical rivers represents a major challenge, particularly where field access is difficult at the best of times. In this paper we have presented two different remote sensing based methods for quantifying key components of the sediment budget in a large remote catchment. While there are still many other aspects of the sediment budget that require quantification, particularly hillslope contributions, colluvial gully erosion, and flood-plain deposition, traditional modelling and dating approaches are probably best suited for these components. However, given the vast extent of alluvial gully erosion (~130 km²) and the highly dynamic channel, with an average annual channel turnover (i.e. new erosion and deposition) of around 5 km² distributed throughout the channel network, a remote sensing approach is the only viable means of quantifying these major components of the sediment budget. The analysis of gully distribution also demonstrates the considerable margin for error when attempting to model sediment contributions based on few field data. However, what this method also demonstrates is a means of accounting for errors and propagating them through the calculations, something rarely done in the published sediment budgeting literature. Accounting for error in this manner provides a framework for better targeting field analysis in order to reduce the overall error margins.

The approach outlined for quantifying bed turnover represents a proof of concept of a remote sensing approach towards the construction of a sediment budget at a whole-catchments scale in a large, remote tropical river. The exercise needs to be repeated at a much higher temporal and spatial resolution to provide a better proxy for actual bed load transport, but even at the resolution applied here (two timeslices 17 years apart) it can provide important insights when broken down spatially. There is clearly a need for additional field evidence to constrain the assumptions regarding the depth of scour and/or deposition within the various geomorphic units. At the sub-catchment scale presented here, clear patterns emerge between the tributaries of differences in sediment accumulation. Such an analysis could be performed at a higher spatial resolution and provide greater insight into patterns of sediment movement through the catchment. The results presented here tend to support the anecdotal observations of a trend towards sediment accretion, and loss of pool area within the lower Mitchell River over the last couple of decades.

REFERENCES

- Aalto, R., Lauer, J. W. & Dietrich, W. E. (2008) Spatial and temporal dynamics of sediment accumulation and exchange along Strickland River floodplains (Papua New Guinea) over decadal-to-centennial timescales. *J. Geophysical Res.-Earth Surface* **113**(F1).
- Brooks, A. P., Knight, J. M. & Spencer, J. (2006) A remote sensing approach for mapping and classifying riparian gully erosion in Tropical Australia. Milestone Report 1 to Land Water Australia for project GRU 37. Australian Rivers Institute, Griffith University, Nathan, Queensland, Australia.
- Brooks, A. P. & Brierley, G. J. (1997) Geomorphic responses of lower Bega River to catchment disturbance, 1851–1926. *Geomorphology* **18**, 291–304.
- Brooks, A. P., Brierley, G. J. & Millar, R.G. (2003) The long-term control of vegetation and woody debris on channel and flood-plain evolution: insights from a paired catchment study in south-eastern Australia. *Geomorphology* **51**, 7–29.
- Brooks, A. P., Shellberg, J. G., Spencer, J. & Knight, J. (2008) Alluvial gully erosion in Northern Australia. *Earth Surf. Processes Landf.* (submitted).
- BRS (1991) Digital Atlas of Australian Soils (Arc/Info® vector format). Originally compiled by K. H. Northcote *et al.* and published in 1960–1968 by CSIRO and Melbourne University Press in Melbourne, known as the *Atlas of Australian Soils*.
- Chappell, J., Rhodes, E. G., Thom, B. G. & Wolanski, E. (1982) Hydro-isostasy and the sea-level isobase of 5500 BP in North Queensland, Australia. *Marine Geology* **49**(1–2), 81–90.

- Crowley, G. M. & Garnett, S. T. (2000) Changing fire management in the pastoral lands of Cape York Peninsula of Northeast Australia, 1623 to 1996. *Australian Geographical Studies* **38**(1), 10–26.
- Dietrich, W. E. & Dunne, T. (1978) Sediment budget for a small catchment in mountainous terrain. *Z. Geomorphol. Suppl.* **29**, 191–206.
- DNRW (2008) <http://www.nrw.qld.gov.au/slats/prod.html>.
- Erskine, W. D. & Green, D. (2000) Geomorphic effects of extractive industries and their implications for river management: the case of the Hawkesbury-Nepean River, New South Wales. In: *River Management: the Australasian Experience* (ed. by S. Brizga & B. Finlayson), 123–150. John Wiley and Sons, Chichester, UK.
- Grimes, K. G. & Douth, H. F. (1978) The late Cainozoic evolution of the Carpentaria Plains, Northern Queensland. *BMR J. Aust. Geol. Geophys.* **3**, 101–112.
- Ham, D. G. & Church, M. (2000) Bed-material transport estimated from channel morphodynamics: Chilliwack River, British Columbia. *Earth Surf. Processes Landf.* **25**(10), 1123–1142.
- Ionita, I. (2006) Gully development in the Moldavian Plateau of Romania. *Catena* **68**(2–3), 133–140.
- Leier, A. L., Decelles, P. G. & Pelletier, J.D. (2005) Mountains, monsoons, and megafans. *Geology* **33**(4), 289–292.
- McDonald, G. T. & Dawson, S. J. (2004) *Northern Gulf region, Natural Resource Management Plan*. Tropical Savannas CRC and NGRMG Ltd., Georgetown, Queensland, Australia.
- Milne, A. K. (1988) Change detection analysis using Landsat imagery: a review of methodology. In: *Proceedings of IGARSS '88 Symposium* (Edinburgh, Scotland, 13–16 September 1988), 541–544.
- Olley, J. M., Murray, A. S., Mackenzie, D. H. & Edwards, K. (1993) Identifying sediment sources in a gullied catchment using natural and anthropogenic radioactivity. *Water Resour. Res.* **29**(4), 1037–1043.
- Platt, R. V. & Rapoza, L. (2008) An evaluation of an object-oriented paradigm for land use/land cover classification. *Professional Geographer* **60**(1), 87–100. Routledge, London, UK.
- Prosser, I. P., Rutherford, I. D., Olley, J. M., Young, W. J., Wallbrink, P. J. & Moran, C.J. (2001) Large-scale patterns of erosion and sediment transport in river networks, with examples from Australia. *Mar. Freshwater Res.* **52**, 81–99.
- Rustomji, P. (2006) Analysis of gully dimensions and sediment texture from southeast Australia for catchment sediment budgeting. *Catena* **67**(2), 119–127.
- Rutherford, I. D. (2000) Some human impacts on Australian stream channel morphology. In: *River Management: The Australasian Experience* (ed. by S. O. Brizga & B. L. Finlayson), 11–50. John Wiley & Sons, Chichester, UK.
- Stanford, J. A., Lorang, M. S. & Hauer, F. R. (2005) The shifting habitat mosaic of river ecosystems. *Verh. Int. Verein. Limnol.* **1**–14.
- van Niekerk, A. W., Heritage, G. L., Broadhurst, L. W. & Moon, B. P. (1999) Bedrock anastomosing channel systems: morphology and dynamics in the Sabie River, Mpumalanga province, South Africa. In: *Varieties of Fluvial Form* (ed. by A. J. Miller & A. Gupta), 33–51. Wiley, Chichester, UK.
- Wallbrink, P. J. (2004) Quantifying the erosion processes and land-uses which dominate fine sediment supply to Moreton Bay, Southeast Queensland, Australia. *J. Environ. Radioactiv.* **76**(1–2), 67–80.
- Whitaker, A. J., Raymond, O. L., Liu, S., Champion, D. C., Stewart, A. J., Retter, A. J., Percival, D. S., Connolly, D. P., Phillips, D. M. & Hanna, A. L. (2006) *Surface Geology of Australia 1:1 000 000 Scale, Eastern States* [Digital Dataset]. The Commonwealth of Australia, Geoscience Australia, Canberra, <http://www.ga.gov.au>.
- Wilkinson, S. N., Prosser, I. P. & Hughes, A. O. (2005) Targeting erosion control in large river systems using spatially distributed sediment budgets. In: *Geomorphological Processes and Human Impacts in River Basins* (ed. by R. J. Batalla & C. Garcia), 56–64. IAHS Publ. 299. IAHS Press, Wallingford, UK.
- Woinarski, J., Mackey, B., Nix, H. & Traill, B. (2007) *The Nature of Northern Australia: its Natural Values, Ecological Processes and Future Prospects*. Australian National University Press, Canberra, Australia.